

CONSTRAINTS ON THE SIZE OF EXTRA DIMENSIONS FROM THE
ORBITAL EVOLUTION OF BLACK-HOLE X-RAY BINARIES

TIM JOHANNSEN

Physics Department, University of Arizona, 1118 E. 4th Street, Tucson, AZ 85721

DIMITRIOS PSALTIS

Physics and Astronomy Departments, University of Arizona,
1118 E. 4th Street, Tucson, AZ 85721

JEFFREY E. MCCLINTOCK

Harvard-Smithsonian Center for Astrophysics, 60 Garden Street, Cambridge, MA 02138

Draft version April 23, 2019

ABSTRACT

One of the plausible unification schemes in physics considers the observable universe to be a 4-dimensional surface (the “brane”) embedded in a higher-dimensional curved spacetime (the “bulk”). In such braneworld gravity models with infinitely large extra dimensions, black holes evaporate through the emission of the additional gravitational degrees of freedom, resulting in lifetimes of stellar-mass black holes that are significantly smaller than the Hubble time. We show that the predicted evaporation rate leads to a change in the orbital period of X-ray binaries harboring black holes that is observable with current instruments. We obtain an upper limit on the rate of change of the orbital period of the binary A0620-00 and use it to constrain the asymptotic curvature radius of the extra dimension to a value comparable to the one obtained by table-top experiments.

Subject headings: gravitation — black hole physics — X-rays: binaries — stars: individual (A0620-00)
— X-rays: stars

1. INTRODUCTION

In the search for the unified theory of all forces, an essential ingredient is the solution of the so-called hierarchy problem. The fundamental scale of gravity, the Planck mass, exceeds the electroweak scale by 16 orders of magnitude. In order to resolve this discrepancy, Arkani-Hamed, Dimopoulos, & Dvali (1998) suggested that gravity is allowed to propagate in more than three spatial dimensions and is hence “diluted” in our universe. This leads to modifications of gravity at distances that are smaller than those probed by experiments. Indeed, Newton’s inverse square law has been tested down to the sub-mm range (Kapner et al. 2007; Geraci et al. 2008), hence verifying that our space is three-dimensional at macroscopic scales. Any modification of gravity involving extra dimensions therefore has to ensure that additional space dimensions only effect our world at distances that are smaller than those experimental limits.

Braneworld gravity offers a solution to this problem in the form of two different scenarios. One approach (Arkani-Hamed et al. 1998) is to compactify n extra dimensions at scales smaller than those set by experiment. The fundamental Planck mass can be pushed down to the electroweak scale of about 1 TeV, provided the extra dimensions are large enough. For n extra dimensions, the limit is $R \lesssim 10^{30/n-17}$ cm. For $n \geq 2$, extra dimensions would have a sub-mm size, which is just at the limit up to which the inverse square law has been verified.

This model, however, cannot be tested in astrophysics, because those length scales are well below astronomical distances.

A second model (Randall & Sundrum 1999) is based on a different idea. The four-dimensional brane with all standard model particles is embedded in an infinite five-dimensional anti-de Sitter space. Deviations from the inverse square law, however, only manifest at distances smaller than the asymptotic curvature radius L of the bulk because the latter is filled with a negative cosmological constant. This setup has dramatic implications for astrophysical black holes.

No stable solutions for black holes on the brane have been found to date. Applying the AdS/CFT correspondence to AdS braneworld models, Emparan, Fabbri, & Kaloper (2002) conjectured that black holes localized on the brane, that are solutions of the classical bulk equations in AdS_{D+1} with the brane boundary conditions, correspond to quantum-corrected black holes in D dimensions. Black holes can then evaporate through the emission of a large number of CFT modes with a lifetime given by (Emparan, García-Bellido, & Kaloper 2003; see, however, Fitzpatrick, Randall, & Wiseman 2006)

$$\tau \sim 1.2 \times 10^2 \left(\frac{M}{M_\odot} \right)^3 \left(\frac{1 \text{ mm}}{L} \right)^2 \text{ yr}, \quad (1)$$

which is only of the order of a hundred thousand years for black-holes with a mass M of a few solar masses and an asymptotic curvature L in the sub-mm range. Therefore, astrophysical black holes can radiate away most of their mass at cosmologically relevant timescales. This prop-

Electronic address: timj@physics.arizona.edu
Electronic address: dpsaltis@physics.arizona.edu
Electronic address: jem@head.cfa.harvard.edu

erty has been used to constrain L from a kinematic limit on the age of the black hole XTE J1118+480 (Psaltis 2007a), yielding $L < 80 \mu\text{m}$, as well as to give a possible explanation of the unusual, observed black-hole mass function (Postnov & Cherepashchuk 2003).

In the Randall-Sundrum model RS2, the gravitational potential at distances close to L takes the form (Randall & Sundrum 1999)

$$V(r) \approx -G \frac{m_1 m_2}{r} \left(1 + \frac{L^2}{r^2} \right). \quad (2)$$

Adelberger et al. (2007) report a 1σ -upper limit on L of $11 \mu\text{m}$. A 3σ -constraint has not been computed yet, but it should be significantly larger and comparable to the 95%-confidence upper bound of $44 \mu\text{m}$ (Kapner et al. 2007) for the size of one compact extra dimension. Hereafter, we will take this as the current experimental constraint on L .

In this paper, we constrain the asymptotic curvature radius L in the RS2 scenario by considering the evaporation of black holes in X-ray binaries. A mass loss of the black hole in the extra dimension leads to an evolution of the orbit, which is potentially measurable. Competing effects are the orbital period evolution due to magnetic braking and the evolution of the companion star (see, e.g., Verbunt 1993). In §2, we systematically derive the rate of change of the orbital period involving all three effects as well as non-conservative mass transfer. We present the results in §3, where we identify systems with predominant black-hole evaporation. In §4 we focus on the black-hole binary A0620-00 in particular and obtain an upper limit of $L < 132 \mu\text{m}$, which is already comparable to the limit from table-top experiments. In the final section (§5) we discuss the potential of this binary as well as of other sources to constrain L down to a few microns.

2. ORBITAL EVOLUTION OF A BLACK-HOLE BINARY IN BRANEWORLD GRAVITY

In this section, we derive the rate of change of the orbital period of a binary system that harbors a black hole following closely the works of Will & Zaglauer (1989) and Psaltis (2007b). In our treatment, we also include the effect of CFT emission of the black hole in the extra dimension.

For a black hole of mass m_1 with a companion star of mass m_2 on a circular orbit, the rate of change of the orbital angular momentum, $J \equiv \mu\sqrt{Gma}$, is

$$\begin{aligned} \frac{\dot{J}}{J} &= \frac{1}{J} \frac{\partial J}{\partial m_1} \dot{m}_1 + \frac{1}{J} \frac{\partial J}{\partial m_2} \dot{m}_2 + \frac{1}{J} \frac{\partial J}{\partial a} \dot{a} \\ &= \left(1 - \frac{1}{2} \frac{m_1}{m_1 + m_2} \right) \frac{\dot{m}_1}{m_1} + \left(1 - \frac{1}{2} \frac{m_2}{m_1 + m_2} \right) \frac{\dot{m}_2}{m_2} + \frac{1}{2} \frac{\dot{a}}{a}, \end{aligned} \quad (3)$$

where $m \equiv m_1 + m_2$, $\mu \equiv m_1 m_2 / m$, and a is the semi-major axis. We set $m_1 = qm_2$ and $\dot{m}_1 = -\beta\dot{m}_2 - \dot{M}$, where \dot{M} is the rate of black-hole evaporation into the higher-dimensional bulk. We then obtain

$$\frac{\dot{J}}{J} = \left(1 - \frac{\beta}{q} - \frac{1}{2} \frac{1-\beta}{1+q} \right) \frac{\dot{m}_2}{m_2} - \left(1 + \frac{1}{2} \frac{q}{1+q} \right) \frac{\dot{M}}{m_1} + \frac{1}{2} \frac{\dot{a}}{a}. \quad (4)$$

Angular momentum may be lost because of mass loss from the system or because of the effect of magnetic braking. This leads to

$$\frac{\dot{J}}{J} = j_w(1-\beta) \frac{1+q}{q} \frac{\dot{m}_2}{m_2} + \frac{\dot{J}_{\text{mb}}}{J}, \quad (5)$$

where j_w is the specific angular momentum carried away by the stellar wind in units of $2\pi a^2/P$, P is the orbital period and \dot{J}_{mb}/J is the rate of angular momentum loss due to magnetic braking. Following Rappaport, Verbunt, & Joss (1983) we estimate the corresponding torque by the empirical expression

$$\tau_{\text{mb}} \equiv \dot{J}_{\text{mb}} \simeq -3.8 \times 10^{-30} m_2 R_\odot^4 \left(\frac{R_2}{R_\odot} \right)^\gamma \omega^3 \text{ dyn cm}. \quad (6)$$

Here, ω is the angular frequency of the secondary, γ is a parameter that characterizes the strength of the magnetic braking, and R_2 is the radius of the stellar Roche lobe which is assumed to be filled at all times (Eggleton 1983),

$$R_2 = \frac{0.49q^{-2/3}}{0.6q^{-2/3} + \ln(1+q^{-1/3})} a. \quad (7)$$

Using the expression for the orbital period

$$\frac{P}{2\pi} = \frac{m}{m_1^3 m_2^3} J^3 G^{-2}, \quad (8)$$

we can evaluate \dot{J}_{mb}/J as

$$\begin{aligned} \frac{\dot{J}_{\text{mb}}}{J} &= C \frac{G(m_1 + m_2)^2}{m_1} \\ &\times \left[\frac{0.49q^{-2/3}}{0.6q^{-2/3} + \ln(1+q^{-1/3})} \right]^\gamma \left[\frac{\sqrt{G(m_1 + m_2)}}{2\pi} P \right]^{\frac{2}{3}(\gamma-5)}, \end{aligned} \quad (9)$$

with

$$C \equiv -3.8 \times 10^{-30} R_\odot^{4-\gamma}. \quad (10)$$

Additionally, from the period equation (8) together with our expressions for m_1 and \dot{m}_1 we find

$$\begin{aligned} \frac{\dot{P}}{P} &= \frac{3}{2} \frac{\dot{a}}{a} - \frac{1}{2} \frac{\beta\dot{m}_2 - \dot{M} + \dot{m}_2}{m_1 + m_2} \\ &= -\frac{1}{2} \frac{1-\beta}{1+q} \frac{\dot{m}_2}{m_2} + \frac{1}{2} \frac{q}{1+q} \frac{\dot{M}}{m_1} + \frac{3}{2} \frac{\dot{a}}{a}. \end{aligned} \quad (11)$$

Using

$$\frac{\dot{q}}{q} = -\frac{\beta+q}{q} \frac{\dot{m}_2}{m_2} - \frac{\dot{M}}{m_1}, \quad (12)$$

we obtain the rate of change of the radius of the companion

$$\begin{aligned} \frac{\dot{R}_2}{R_2} &= \frac{\dot{a}}{a} + \frac{2}{3} \frac{\beta+q}{q} \left[1 - \frac{0.6 + 0.5q^{1/3}(1+q^{-1/3})^{-1}}{0.6 + q^{2/3} \ln(1+q^{-1/3})} \right] \frac{\dot{m}_2}{m_2} \\ &\quad + \frac{2}{3} \left[1 - \frac{0.6 + 0.5q^{1/3}(1+q^{-1/3})^{-1}}{0.6 + q^{2/3} \ln(1+q^{-1/3})} \right] \frac{\dot{M}}{m_1}. \end{aligned} \quad (13)$$

The third effect that dictates the change of the orbital period in a binary system is the evolution of the companion star. As the secondary leaves the main sequence and starts to burn helium, it expands rapidly. Following Webbink, Rappaport, & Savonije (1983) and Verbunt (1993) we estimate the rate of change of the radius of a star leaving the main sequence as

$$\left(\frac{\dot{R}_2}{R_2}\right)_{\text{ev}} = (c_1 + 2c_2y + 3c_3y^2) \frac{\dot{M}_c}{M_c}. \quad (14)$$

Here, M_c is the core mass of the companion, $y \equiv \ln(M_c/0.25M_\odot)$, and c_1 , c_2 and c_3 are constants that depend on the composition of the core. The core mass changes in time according to (Verbunt 1993)

$$\dot{M}_c \simeq 1.37 \times 10^{-11} \left(\frac{L_2}{L_\odot}\right) M_\odot \text{yr}^{-1}. \quad (15)$$

In this expression, L_2 is the luminosity of the companion, which is determined by the core mass (Webbink et al. 1983) according to the empirical relation

$$\ln\left(\frac{L_2}{L_\odot}\right) = a_0 + a_1y + a_2y^2 + a_3y^3, \quad (16)$$

with a_0 , a_1 , a_2 , and a_3 constants depending on the core composition. Combining equations (14) – (16) leads to

$$\begin{aligned} \left(\frac{\dot{R}_2}{R_2}\right)_{\text{ev}} &\simeq 1.37 \times 10^{-11} \times 4^{a_1} (c_1 + 2c_2y + 3c_3y^2) \\ &\times e^{a_0 + a_2y^2 + a_3y^3} \left(\frac{M_c}{M_\odot}\right)^{a_1-1} \text{yr}^{-1}. \end{aligned} \quad (17)$$

We now define the adiabatic index for the companion star as

$$\xi_{\text{ad}} \equiv \frac{d \ln R_2}{d \ln m_2} \quad (18)$$

and obtain

$$\begin{aligned} \frac{\dot{a}}{a} &= \left[\xi_{\text{ad}} - \frac{2}{3} \frac{\beta + q}{q} \left(1 - \frac{0.6 + 0.5q^{1/3}(1 + q^{-1/3})^{-1}}{0.6 + q^{2/3} \ln(1 + q^{-1/3})} \right) \right] \frac{\dot{m}_2}{m_2} \\ &- \frac{2}{3} \left[1 - \frac{0.6 + 0.5q^{1/3}(1 + q^{-1/3})^{-1}}{0.6 + q^{2/3} \ln(1 + q^{-1/3})} \right] \frac{\dot{M}}{m_1} - \left(\frac{\dot{R}_2}{R_2}\right)_{\text{ev}}. \end{aligned} \quad (19)$$

In the following we will estimate the value of ξ_{ad} from the expressions for the stellar radius R and mass m_2 given by Kalogera & Webbink (1996).

Combining the equations we derived above, we obtain the rate of change of the orbital period of the binary

$$\begin{aligned} \frac{\dot{P}}{P} &= Q_0 \frac{\dot{M}}{m_1} + Q_2 \frac{(m_1 + m_2)^2}{m_1} \\ &\times \left[\frac{0.49q^{-2/3}}{0.6q^{-2/3} + \ln(1 + q^{-1/3})} \right]^\gamma \left[\frac{\sqrt{G(m_1 + m_2)}}{2\pi} P \right]^{\frac{2}{3}(\gamma-5)} \\ &+ Q_3 (c_1 + 2c_2y + 3c_3y^2) e^{a_0 + a_2y^2 + a_3y^3} \left(\frac{M_c}{M_\odot}\right)^{a_1-1}. \end{aligned} \quad (20)$$

In this equation we have introduced the quantities

$$\begin{aligned} Q_0 &\equiv \frac{1}{2} \frac{1 - \beta}{1 + q} \frac{1 + \frac{1}{2} \frac{q}{1+q} + \frac{1}{3} \mathcal{A}}{D} + \frac{1}{2} \frac{q}{1 + q} \\ &+ \frac{3}{2} \frac{\left(\frac{2}{3} \frac{\beta+q}{q} \mathcal{A} - \xi_{\text{ad}}\right) \left(1 + \frac{1}{2} \frac{q}{1+q} + \frac{1}{3} \mathcal{A}\right)}{D} - \mathcal{A}, \end{aligned} \quad (21)$$

$$Q_2 \equiv \frac{C}{D} G \left(\frac{1}{2} \frac{1 - \beta}{1 + q} + \frac{\beta + q}{q} \mathcal{A} - \frac{3}{2} \xi_{\text{ad}} \right), \quad (22)$$

$$\begin{aligned} Q_3 &\equiv 1.37 \times 10^{-11} \times 4^{a_1} \\ &\times \left[\frac{1}{4D} \frac{1 - \beta}{1 + q} + \frac{1}{2D} \left(\frac{\beta + q}{q} \mathcal{A} - \frac{3}{2} \xi_{\text{ad}} \right) - \frac{3}{2} \right], \end{aligned} \quad (23)$$

$$\mathcal{A} \equiv 1 - \frac{0.6 + 0.5q^{1/3}(1 + q^{-1/3})^{-1}}{0.6 + q^{2/3} \ln(1 + q^{-1/3})}, \quad (24)$$

and

$$D \equiv j_w(1 - \beta) \frac{1 + q}{q} - 1 + \frac{\beta}{q} + \frac{1}{2} \frac{1 - \beta}{1 + q} - \frac{1}{2} \left(\xi_{\text{ad}} - \frac{2}{3} \frac{\beta + q}{q} \mathcal{A} \right). \quad (25)$$

For the “evaporation” of the black hole due to the emission of CFT modes, which are the dual description of the infinite dimension, we use (Emparan et al. 2003)

$$\dot{M} = -2.8 \times 10^{-3} \left(\frac{M_\odot}{m_1}\right)^2 \left(\frac{L}{1 \text{ mm}}\right)^2 M_\odot \text{yr}^{-1}, \quad (26)$$

where L is the asymptotic AdS radius of curvature. Defining

$$Q_1 \equiv -2.8 \times 10^{-3} Q_0 \text{yr}^{-1}, \quad (27)$$

we arrive at our final equation for the orbital period evolution:

$$\begin{aligned} \frac{\dot{P}}{P} &= Q_1 \left(\frac{M_\odot}{m_1}\right)^3 \left(\frac{L}{1 \text{ mm}}\right)^2 \\ &+ Q_2 \frac{(m_1 + m_2)^2}{m_1} \left[\frac{0.49q^{-2/3}}{0.6q^{-2/3} + \ln(1 + q^{-1/3})} \right]^\gamma \\ &\times \left[\frac{\sqrt{G(m_1 + m_2)}}{2\pi} P \right]^{\frac{2}{3}(\gamma-5)} \\ &+ Q_3 (c_1 + 2c_2y + 3c_3y^2) e^{a_0 + a_2y^2 + a_3y^3} \left(\frac{M_c}{M_\odot}\right)^{a_1-1}. \end{aligned} \quad (28)$$

3. RESULTS

In this section, we investigate the potential of the currently known black-hole binary systems to constrain the rate of black-hole evaporation into higher dimensions. We will start with a general discussion of the various systems and then focus on the system A0620-00 in particular.

First we investigate which term in equation (28) dominates the period evolution for a given period P , black hole and companion masses m_1 , m_2 , respectively, and curvature radius L . Figure 1 shows the orbital periods versus the companion masses of the observed systems. On the same graph we plot the curves along which the

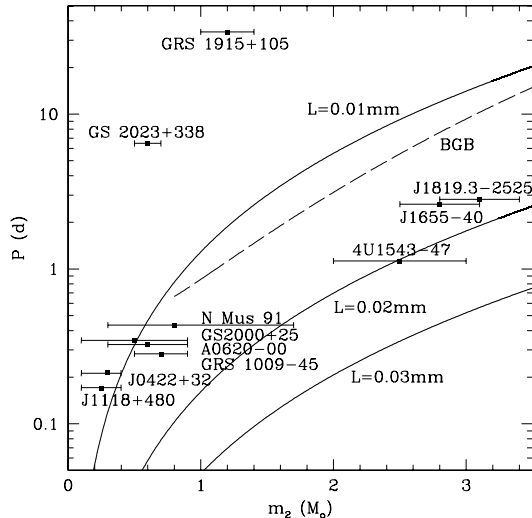


FIG. 1.— The orbital period P of observed black-hole binary systems versus the mass m_2 of the companion star. Three separatrices are shown for different values of the asymptotic AdS curvature radius L for a nominal black-hole mass of $10M_\odot$. Below the lines, the magnetic braking dominates. Above the lines, the black-hole evaporation dominates. Binaries above the curve marked BGB contain companions beyond the base of the giant branch; for these systems, the evolution of the companion completely dominates the orbital evolution of the binary. The parameters for this graph are $\xi_{\text{ad}} = 0.8$, $\beta = 0$, $j_w = 0$, and $\gamma = 4$.

evaporation term equals the magnetic braking term for $L = 0.01$ mm, $L = 0.02$ mm, and $L = 0.03$ mm. The evaporation dominates above the lines, whereas below the lines the magnetic braking dominates. Recent numerical simulations (Yungelson & Lasota 2008) showed that the expression for magnetic braking is actually overestimated for low-mass black-hole binaries, which further increases the predominance of the evaporation term. The parameters we used in this figure are $\xi_{\text{ad}} = 0.8$, $\beta = 0$, $j_w = 0$, and $\gamma = 4$, and we set the black-hole mass to a nominal value of $10M_\odot$.

For companion masses $\gtrsim 1M_\odot$, there exists a maximum period beyond which systems contain companion stars that have evolved past the base of the giant branch (see the curve marked BGB in Figure 1). For these systems, the evolution of the companion star completely dominates the rate of change of the orbital period for any plausible value of the asymptotic curvature L .

We find that two sources have relatively large orbital periods and are probably evolved, while the other systems group around the lines that correspond to $L = 0.02$ mm and $L = 0.01$ mm, respectively. Among the latter we identify the system A0620-00 as a prime candidate both because of the theoretical expectation shown in this figure and because of the extensive historical monitoring of its orbital period. We analyze this source more closely in the following.

The short-period (0.32 d) binary A0620-00 has a secondary that resembles a main sequence star, as indicated by its spectrum and by its chemical abundances (González Hernández et al. 2004). Its mass and radius are also comparable to that of a main-sequence K4 star (Marsh et al. 1994). In particular, the mean density of this Roche-lobe-filling secondary, which is precisely determined by its orbital period (Frank et al. 2002), is only

Table 1: Observed Properties of X-Ray Binaries^a

X-Ray Binary	P (h)	q	m_1 (M_\odot)
GRS1915+105	816	12	14 ± 4
J1118+480	4.1	~ 20	6.8 ± 0.4
GS2023+338	155.3	17 ± 1	12 ± 2
GS2000+25	8.3	24 ± 10	10 ± 4
H1705-25	12.5	> 19	6 ± 2
GRS1009-45	6.8	7 ± 1	5.2 ± 0.6
N Mus 91	10.4	6.8 ± 2	6^{+5}_{-2}
A0620-00	7.8	17 ± 1^b	10 ± 5
J0422+32	5.1	$9.0^{+2.2}_{-2.7}$	4 ± 1
J1819.3-2525	67.6	2.31 ± 0.08	7.1 ± 0.3
J1655-40	62.9	2.39 ± 0.15	6.6 ± 0.5
4U1543-47	27.0	3.6 ± 0.4	9.4 ± 1

^aMost data compiled by Charles & Coe (2006)

^bNeilsen, Steeghs & Vrtilik (2008)

$\sim 25\%$ below that of a normal K4 dwarf. However, the secondary of A0620-00 is not a normal star, given the extraordinary evolutionary history of this black-hole binary system (e.g., de Kool et al. 1986). Nevertheless, for our purposes the secondary functions like a main sequence star: it is not evolving on a nuclear time scale and the system is kept in contact by magnetic braking (Justham et al. 2006).

Thus we can neglect the evolution term in equation (28) and plot the expected rate of change of its orbital period P as a function of the asymptotic AdS curvature radius L (see Figure 2). The parameters for this plot are $\beta = 0$, $j_w = 0$, $\gamma = 4$, and $\xi_{\text{ad}} = 0.8$. We see that for $L \lesssim 10 \mu\text{m}$ the magnetic braking dominates and the rate of orbital period change is constant because it is independent of L . For $L \gtrsim 10 \mu\text{m}$ the black-hole evaporation dominates and the orbital period derivative increases with decreasing AdS curvature as expected. This shows that A0620-00 theoretically allows for a constraint on L down to $10 \mu\text{m}$, assuming that $m_1 = 10M_\odot$. Since m_1 has only been measured to an accuracy of $\pm 50\%$, the constraint on L can even be reduced to a few microns because of the dependence of the rate of change of the orbital period on the mass of the primary. We will return to the question of the black-hole mass in the next section.

In order to determine the dependence of the orbital period evolution on the parameters j_w , β , and γ , we plot the rate of change of the orbital period as a function of one parameter while holding the others constant. In all plots, we set $\xi_{\text{ad}} = 0.8$ (estimated from Kalogera & Webbink 1996) for the companion mass in this system and evaluate the period evolution rate at the current experimental upper limit of the AdS curvature of $L = 44 \mu\text{m}$ (Kapner et al. 2007). Figure 3 shows the dependence of the rate of change of the orbital period on the parameters j_w , β , and γ , respectively. First we note that for large values of the parameters the period decreases. This behavior is entirely due to the high mass ratio $q = m_1/m_2$ measured for this source; for other sources with substantially smaller mass ratios, the behavior is not monotonic. Furthermore, we find that the modulus of the rate of change of the orbital period is the smallest when $j_w = 0$ (no angular momentum loss due to stellar wind), $\beta = 0$ (no accretion), and $\gamma = 4$. We choose these values for the respective parameters in the following discussion, where we are aiming to calculate a lower limit on the expected rate of change of the orbital period of the binary system

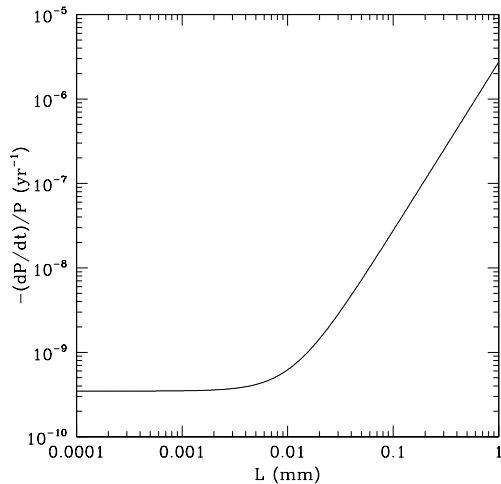


FIG. 2.— The rate of change of the orbital period P of the binary system A0620-00 versus the asymptotic curvature radius L in the extra dimension. The parameters are $\xi_{\text{ad}} = 0.8$, $\beta = 0$, $j_w = 0$, and $\gamma = 4$. The transition from predominant magnetic braking (constant rate) to predominant black-hole evaporation (linearly increasing rate) occurs at $L \simeq 10 \mu\text{m}$ for this set of parameters.

A0620-00.

4. DATA

In this section we use previously published measurements of the orbital period of A0620-00 to set an upper limit on the size L of the asymptotic curvature in the extra dimension. First we determine that limit using the best fit black-hole mass of $m_1 = 10M_\odot$, then we proceed with an analysis of L for different black-hole masses.

The orbital period of A0620-00 ($P = 0.32$ d) has been measured several times during the past two decades. A convenient orbital phase reference is the time of maximum radial velocity T_0 . Four measured values of T_0 , which span 22 years, are given in Table 2. These times and the individual determinations of the orbital period P uniquely determine the cycle number n . The table also gives the calculated times of maximum velocity based on a simple ephemeris with a constant orbital period and referenced to the most precise and recent determination of T_0 (see footnote *a* of Table 2). The differences between the observed and calculated times are smaller than their corresponding uncertainties, and thus there is no evidence for any change in the orbital period during the past 22 years. Note that with modern telescopes and instrumentation one can routinely achieve a precision of several seconds in T_0 (see the last entry in the table) in ~ 10 hours of radial velocity observations of a source like A0620-00 (Neilsen et al. 2008).

Of interest to us is a secure limit on the rate of change of the orbital period. A constant rate of change of the period will result in a quadratic variation in T_0 (e.g., Kelley et al. 1983). The time of the n th value of T_0 is then given by

$$t_n = t_0 + Pn + \frac{1}{2}P\dot{P}n^2, \quad (29)$$

where P and \dot{P} are the orbital period and its derivative, respectively, at time t_0 ; n is the orbital cycle number.

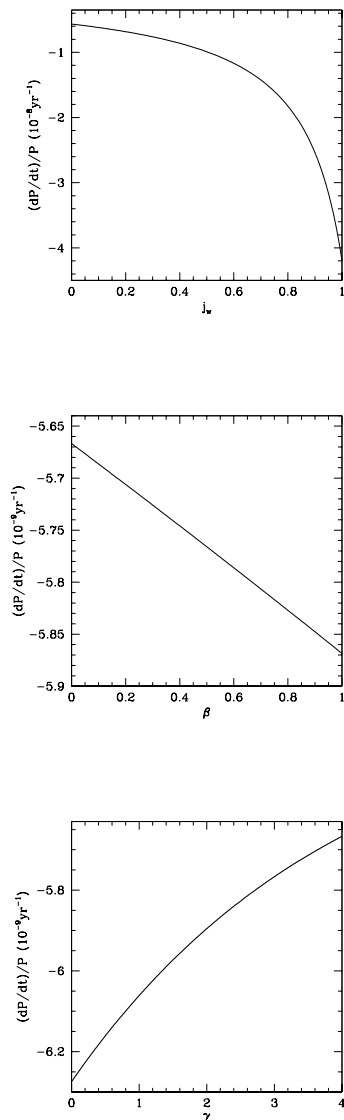


FIG. 3.— The rate of change of the orbital period P (in years) of the binary system A0620-00 versus the specific angular momentum removed by the wind j_w , the accretion parameter β , and the magnetic braking parameter γ , for $L = 44 \mu\text{m}$ and $\xi_{\text{ad}} = 0.8$. On varying one parameter, the others are held constant at the respective values $j_w = 0$, $\beta = 0$, and $\gamma = 4$.

Following the standard procedure and using the IDL routine *curvefit*, we fitted for the three parameters t_0 , P and \dot{P} using the four observed values of T_0 given in Table 2 (Figure 4). The fit yields $\dot{P} = (1.66 \pm 2.64) \times 10^{-11}$ s/s. Thus, using a 3σ -upper limit, the modulus of the period derivative cannot exceed 9.6×10^{-11} s/s. Next we plot the rate of change of the orbital period versus the AdS curvature for the values of the parameters β , j_w , and γ that lead to the lowest limit of the rate of change of the orbital period. Since the measured upper limit on the period derivative in equation (29) marks the largest time change of the orbital period, the intersection point of these two lines places an upper limit of $L \leq 132 \mu\text{m}$

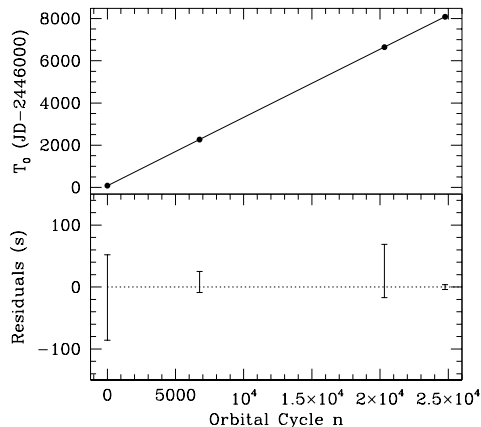


FIG. 4.— The time of maximum radial velocity T_0 and residuals versus the orbital cycle number n for the binary A0620-00.

(Figure 5).

Since the upper limit on the asymptotic curvature radius depends strongly on the black-hole mass, which has only been measured to an accuracy of $\pm 50\%$, we plot in Figure 6 the upper limit L_{\max} versus the black-hole mass for different limits on the period change. For the upper curve we used the current limit on the orbital period evolution from the fit using equation (29), whereas for the lower curve we used a value that is a factor of 10 lower. We see that even the current table-top limit of the asymptotic AdS curvature radius $L = 44 \mu\text{m}$ can be improved if the upper limit of the rate of change of the orbital period can be reduced to 10% of the current value and if the black-hole mass is smaller than $10M_\odot$.

There are ample opportunities to substantially improve the above limit on L using our method. For example, because the uncertainty in \dot{P} depends quadratically on n , even a single future observation of A0620-00 that extends the 22-year baseline by just 5 years (i.e., $n = 30423$) with a precision of 4 s would reduce the error in \dot{P} by a factor of six. Furthermore, independent limits of comparable quality on \dot{P} and L could be obtained by monitoring the ephemerides of several other black-hole binary systems (e.g., GRS 1124-683, XTE J1118+480 and 4U 1543-47; Remillard & McClintock 2006).

A very exciting aspect of our method is that it not only allows us to constrain the AdS radius L , but also to actually measure it, provided that the measurement of the rate of change of the orbital period yields a value with modulus larger than $8 \times 10^{-8} \text{ yr}^{-1}$. In Figure 5 we used the set of the parameters β , γ , and j_w that corresponds to the smallest period evolution for a given L . We can also plot the rate of change of the orbital period as a function of L for the set $\beta = 1$, $\gamma = 0$, $j_w = 1$, which places an upper limit on the period evolution. Hence any measured value of the rate of change of the orbital period has to lie between the two curves, as shown in Figure 7 for black-hole masses $m_1 = 5, 10$, and $15M_\odot$. Since our method is model-dependent (RS2), such a measurement, together with the table-top experiments, would even allow for a distinction between the ADD and the RS2 scenario. Cur-

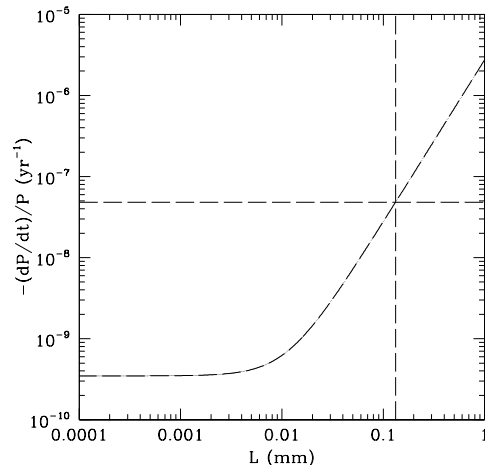


FIG. 5.— The lower limit on the rate of change of the orbital period P of the binary system A0620-00 as a function of the asymptotic AdS curvature radius L for a black-hole mass of $10M_\odot$. The observed upper limit of the orbital period derivative is shown as a horizontal line. The intersection point marks our constraint on the asymptotic curvature in the bulk of $L = 132 \mu\text{m}$ (vertical line).

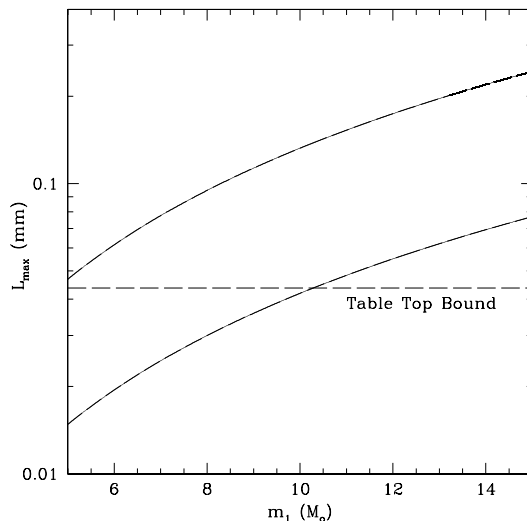


FIG. 6.— The upper limit on the asymptotic AdS curvature radius L as a function of the black hole mass m_1 of A0620-00 using the current lower limit on the orbital period evolution (upper curve) and on 10% of that limit (lower curve). The dashed line shows the current upper limit on L from table-top experiments.

rent table-top experiments, that probe Newton's inverse square law in the sub-mm range, are insensitive to the underlying model, so that their results together with a measurement as discussed above would indeed allow for a distinction between ADD and RS2.

5. DISCUSSION

For a binary system consisting of a black hole and a companion star we derived the rate of change of the orbital period in the RS2 braneworld gravity model incorporating the emission of CFT modes in the extra dimension. Magnetic braking and the evolution of the compan-

Table 2: Observed and Computed Heliocentric Times of Maximum Velocity for A0620-00

Orbital Cycle n	T_0 in JD observed	$T_0(n)$ in JD ^a computed	$T_0 - T_0(n)$ (s)	Reference ^b
(1)	(2)	(3)	(4)	(5)
0	2,446,082.7481 \pm 0.0008	2,446,082.7483	-17 ± 69	1
6764	2,448,267.6155 \pm 0.0002 ^c	2,448,267.6154	8 ± 17	2
20321	2,452,646.7173 \pm 0.0005	2,452,646.7170	26 ± 43	3
24773	2,454,084.77560 \pm 0.00005	2,454,084.77560	0 ± 4	4

$$^a T_0(n) = \text{JD } 2,454,084.77560 - (24773 - n) \times 0.32301406.$$

^bREFERENCES: (1) McClintock & Remillard 1986; (2) Orosz et al. 1994; (3) Shahbaz et al. 2004; (4) Neilsen et al. 2007.

^c T_0 corrected to date of observation on 1991 January 11 using ephemeris in reference (1).

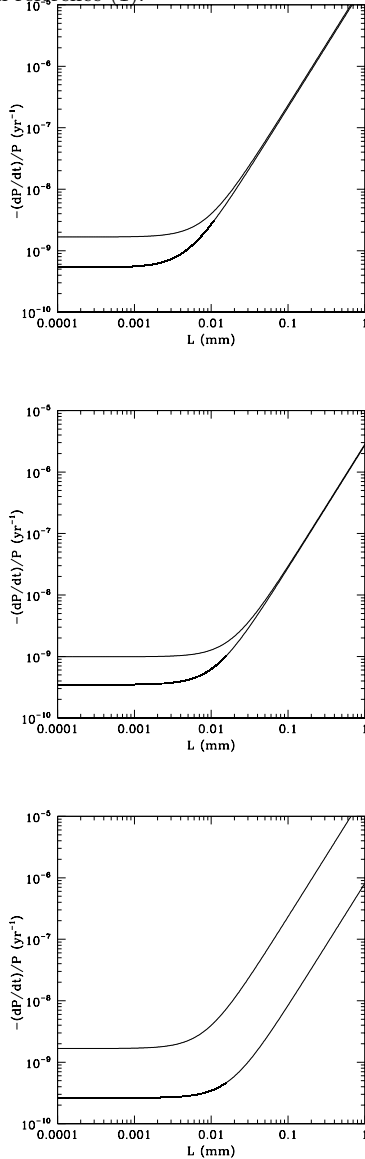


FIG. 7.— The maximum (upper curve) and minimum (lower curve) rate of change of the orbital period of the binary A0620-00 versus the asymptotic AdS curvature radius L for $m_1 = 5, 10, 15M_\odot$, respectively. Any value of the period evolution has to lie between the curves, which allows for a measurement of L if $-\dot{P}/P \gtrsim 8 \times 10^{-8} \text{ yr}^{-1}$.

ion star can also change the orbital period, but they are negligible if the secondary is a main-sequence star and if the asymptotic AdS curvature radius L is large enough so that the evaporation dominates. Measuring the rate of change of the orbital period then allows us to constrain the asymptotic AdS curvature radius.

We analyzed in detail the binary system A0620-00 which is a good candidate for such a constraint for both theoretical and observational reasons. The evaporation term dominates the change of the orbital period as long as the asymptotic curvature radius is at least a few microns large. Measurements of the orbital period over the last 20 years allow for a constraint of $L \leq 132 \mu\text{m}$ assuming a black-hole mass of $10M_\odot$. Refining the measurement of the mass of the black hole and of the rate of change of the orbital period can further improve the constraint on the asymptotic curvature radius. As an example we showed that improving the measurement of the rate of change of the orbital period by one order of magnitude will constrain the AdS curvature radius to a value smaller than the current experimental limit $L = 44 \mu\text{m}$ (Kapner et al. 2007), provided the black-hole mass is measured not to exceed $10M_\odot$.

Considering the other known black-hole X-ray binaries, we see from Figure 1 that there are more systems which we can use in constraining the asymptotic curvature radius in the extra dimension. The requirement of unevolved secondaries rules out some of them, but those grouped around the analyzed source A0620-00 also have the potential of a constraint on the curvature radius down to a few microns.

We would like to thank Nemanja Kaloper and Keith Dienes for fruitful discussions as well as Jack Steiner for his help with the IDL *curvefit* calculations. We also thank Saul Rappaport for his input on issues of black-hole binary evolution. This work was supported in part by the NSF CAREER award NSF 0746549.

REFERENCES

- Adelberger, E. G., Heckel, B. R., Hoedl, S., Hoyle, C. D., & Kapner, D. J. 2007, PRL 98, 131104
- Arkani-Hamed, N., Dimopoulos, S. & Dvali, G. 1998, Phys. Lett. B 429, 263

- Charles, P. A., Coe, M. J., in "Compact Stellar X-ray Sources", eds. W.H.G. Lewin and M. van der Klis (Cambridge University Press), arXiv:0308020
- de Kool, M., van den Heuvel, E. P. J., Pylyser, E. 1987, 1987, A&A, 183
- Eggleton, P. P. 1983, ApJ, 268, 368
- Emparan, R., Fabbri, A., & Kaloper, N. 2002, JHEP 0208, 043
- Emparan, R., García-Bellido, J., & Kaloper, N. 2003, JHEP 0301, 079
- Fitzpatrick, A. L., Randall, L., & Wiseman, T. 2006, JHEP 0611, 033
- Frank, J., King, A. R., & Raine D. 2002, Accretion Power in Astrophysics (Cambridge University Press)
- Geraci, A. A., Smullin, S. J., Weld, D. M., Chiaverini, J., & Kapitulnik, A. 2008, Phys. Rev. D in press, arXiv:0802.2350.v1
- González Hernández, J. I., Rebolo, R., Israelian, G., & Casares, J. 2004, ApJ, 609, 988
- Justham, S., Rappaport, S., & Podsiadlowski, P. 2006, MNRAS, 366, 1415
- Kalogera, V., & Webbink, R. F. 1996, ApJ, 458, 301
- Kapner, D. J., Cook, T. S., Adelberger, E. G., Gundlach, J. H., Heckel, B. R., Hoyle, C. D., & Swanson, H. E. 2007, Phys. Rev. Lett. 98, 021101
- Kelley, R. L., Rappaport, S., Clark, G. W., & Petro, L. D. 1982, ApJ, 268, 790
- Marsh, T. R., Robinson, E. L., & Wood, J. H. 1994, MNRAS, 266, 137
- McClintock, J. E., & Remillard, R. A. 1986, ApJ, 308, 110
- Murdin, P., Allen, D. A., Morton, D. C., Whelan, J. A. J., & Thomas, R. M. 1980, MNRAS 192, 709
- Neilsen, J., Steeghs, D., & Vrtilek, S. D. 2008, MNRAS in press, arXiv:0710.3202
- Oke, J. B. 1977, ApJ, 217, 181
- Orosz, J. A., Bailyn, C. D., Remillard, R. A., McClintock, J. E., & Foltz, C. B. 1994, ApJ, 436, 848
- Postnov, K. A., & Cherepashchuk, A. M. 2003, Astron. Rep. 80, 1075
- Psaltis, D. 2007a, Phys. Rev. Lett. 98, 181101
- Psaltis, D. 2007b, ApJ in press, arXiv:0501234
- Randall, L., & Sundrum, R. 1999, Phys. Rev. Lett. 83, 4690
- Rappaport, S., Verbunt, F., & Joss, P. C. 1983, ApJ, 275, 713
- Remillard, R. A., & McClintock, J. E. 2006, ARAA, 44, 49
- Shahbaz, T., Hynes, R. I., Charles, P. A., Zurita, C., Casares, J., Haswell, C. A., Araujo-Betancor, S., & Powell, C. 2004, MNRAS, 345, 31
- Verbunt, F. 1993, ARAA 31, 93
- Webbink, R. F., Rappaport, S., & Savonije, G. J. 1983, ApJ, 270, 678
- Will, C. M., & Zaglauer, H. W. 1989, ApJ, 346, 366
- Yungelson, L., & Lasota, J.-P., to appear in New Astronomy Review, Proceedings of "Jean-Pierre Lasota, X-ray binaries, accretion disks and compact stars", ed. M. Abramowicz, arXiv:0801.3433v2